ELSEVIER

Contents lists available at ScienceDirect

Journal of Magnetism and Magnetic Materials

journal homepage: www.elsevier.com/locate/jmmm





Domain wall velocity asymmetries driven by saturation magnetization gradients without a Dzyaloshinskii-Moriya interaction

Trae L. Staggers, Livan Jacob, Shawn D. Pollard

Department of Physics and Materials Science, University of Memphis, Memphis, TN 38152, USA

ARTICLE INFO

Keywords: Nanomagnetism Spintronics Thin films Chirality Micromagnetics

ABSTRACT

The discovery of asymmetric domain wall velocities in magnetic alloys and multilayers without a heavy metal underlayer has given rise to claims of a large Dzyaloshinskii-Moriya interaction (DMI) driven by compositional non-uniformities. However, these non-uniformities also give rise to vertically non-uniform magnetic properties which can influence the dynamic properties of domain walls. In this work, we use micromagnetic simulations to show that vertical modulation of the saturation magnetization can give rise to asymmetric domain wall velocities for field and current driven motion, closely resembling the presence of a DMI. For field driven motion, by comparing the velocity asymmetries for varying saturation magnetization gradients, film thicknesses, and average saturation magnetization, we show that the magnitude of effective symmetry breaking field resulting from the non-uniformity can be comparable to those resulting from DMI. These effects scale with thickness and degree of modulation, mirroring recent results in single layer materials. However, the scaling of domain velocity asymmetries is largely suppressed for SOT driven domain dynamics. Therefore, great care needs to be taken when evaluating DMI in non-uniform systems.

1. Introduction

The dynamics of chiral spin textures, including homochiral Néel walls [1], magnetic skyrmions [2-8], and higher order excitations [9-12], have seen an explosion of interest due to their potential applications in a variety of spintronic devices [13-15]. These textures are typically the result of an antisymmetric exchange interaction which breaks the degeneracy between opposing spin chiralities, known as the Dzyaloshinskii-Moriya interaction (DMI) [16-18]. In traditional heavy metal/ferromagnetic bilayers and multilayers, DMI results from spinorbit coupling and broken inversion symmetry at interfaces [19-24]. In ultrathin films with weak demagnetization energies and strong perpendicular magnetic anisotropy, this interfacial DMI (iDMI) can result in Néel-type spin structures, where the magnetization rotates between out-of-plane directions orthogonal to the domain boundary [1,25-27], as opposed to films lacking DMI, in which Bloch walls are favored. In thicker materials, however, a two-dimensional description of the domain wall fails as demagnetization energies combined with DMI can result in a non-uniform spin structure through the film thickness, characterized by an achiral Bloch component and a chiral Néel component governed by the sign of iDMI. It has been demonstrated that this modified structure plays a key role in the static and dynamic properties of chiral domain walls, including determining domain wall velocities and their interactions with defects [3,28-30].

Recently, it has also been suggested that composition gradients in magnetic films can lead to a notable DMI with identical symmetry to that of iDMI, even in nominally symmetric multilayers and alloys without clear interfaces [31-34]. The magnitude of the observed DMI was shown to scale with total film thicknesses, up to an observed effective iDMI on the order of $100\,\mu J/m^2$, comparable to that found in ultrathin heavy metal/ferromagnetic bilayers. This DMI plays a key role in spin-torque driven magnetization dynamics, and as such understanding its origin and scaling in inhomogeneous films is crucial for their use in a variety of device architectures. Due to its relatively small magnitude, understanding extrinsic effects which may influence magnetic states in similar ways is crucial towards the accurate determination of gradient driven DMI.

One complication when attempting to extract information from nonuniform magnetic structures, including potential gradient driven DMI is the need to separate the effects of non-uniform magnetic properties due to inhomogeneities along the film's vertical axis, including differences in exchange stiffness, saturation magnetization, and anisotropy.

E-mail address: shawn.pollard@memphis.edu (S.D. Pollard).

^{*} Corresponding author.

Understanding the role these non-uniformities play in the static and dynamic properties of three-dimensional spin textures is essential towards the realization of devices whose functionalities are intrinsically tied to their spin structure, which determines both static and dynamic properties. Here, we use micromagnetic simulations to understand the influence of varying saturation magnetization through a film's vertical axis on the dynamic behavior of domain walls confined to nanowire geometries. We find that the domain wall dynamics exhibit similar behavior to that of multilayers with moderate iDMI. The magnitude of the asymmetry in velocities scales with both the degree of variation in Ms and the total film thickness. The resulting asymmetries in velocity are of similar magnitude of these recent results which have suggested the presence of DMI in compositionally modulated ferrimagnets [31,32].

Methods.

Micromagnetic modelling of domain wall velocities in a nanowire was carried out using MuMax3 [35,36]. The nanowire geometry was chosen with dimensions of $1024 \, nm \times 256 \, nm \times t$, where t is the film thickness in nanometers. The nanowire was discretized into $512 \times$ $128 \times N$ cells and N = 5, 10, or 21 cells for t = 10, 20 and 40 nm thick wires, respectively. To exclude edge effects during domain wall motion, the simulation window was dynamically shifted such that the domain wall remained in the center, approximating an infinitely long wire. Material parameters were chosen to be consistent with standard Cobased multilayers and alloys [31,32,34,37]. The average saturation magnetization was allowed to vary between $M_s = 200 - 400 \, kA/m$. These limits were chosen such that the domain boundary will not deform significantly during application of external fields or spin currents. For all simulations, we use a damping $\alpha = 0.1$, an exchange stiffness $A_{ex} =$ $10 \, pJ/m$, and a uniaxial anisotropy $K_u = 4.0 \times 10^5 \, J/m^3$. Composition gradients were modeled as a linearly varying M_s through the film thickness, with the center cell equal to the average M_s . In our notation, films are labelled as $M_s \pm \delta$, where δ denotes the degree of variation, i.e. a film with variation from $M_s = 500 \, kA/m$ at the base cell to $M_s =$ $300 \, kA/m$ at the top cell is denoted as $M_s = 400 \pm 100 \, kA/m$. For the opposite gradient, δ is negative. The thickness dependence of the magnetization may be expressed as.

$$(M_n) = (M_s + \delta) - \frac{2n\delta}{N-1} \tag{1} \label{eq:mass}$$

where n is the index of the cell along the thickness direction and ranges from 0 to N -1 and M_n is the magnetization of the n-th cell. The degree of variation used in this work is consistent with composition variations of only a few percent in the low M_s regime for a variety of previously explored ferrimagnets [32,38].

To study the influence of the composition gradient on asymmetric domain wall motion, the wire was initialized in a two-domain state with an in-plane field H_x applied along a wire's long axis. The magnetization was then allowed to relax to generate an initial magnetic configuration, resulting in a static metastable domain boundary centered in the simulation window. Of note, due to the thickness of the films, the Bloch component of the DW chirality may point along the positive or negative y-axis at low in-plane fields. We label domain walls by their Bloch chirality as CW and CCW for an initial Bloch component aligned along the wire's positive or negative y-axis respectively. All low-field simulations were carried out utilizing both Bloch chiralities to account for any differences arising from this chirality, including dynamic effects resulting in a preferred Bloch chirality in combination with in-plane fields for thick magnetic films [39].

Subsequently an out of plane magnetic field $H_z=2.5\,\mathrm{mT}$ was applied to drive domain wall motion, as shown schematically in Fig. 1(a). The value of H_z was chosen to limit switching of the Bloch chirality at low inplane fields due to dynamic effects. To avoid the influence of the initial domain wall acceleration phase, the initial 5 ns of simulation time was excluded from the results. Total runs for each field value varied between 25 and 100 ns, depending on the difference in velocities between

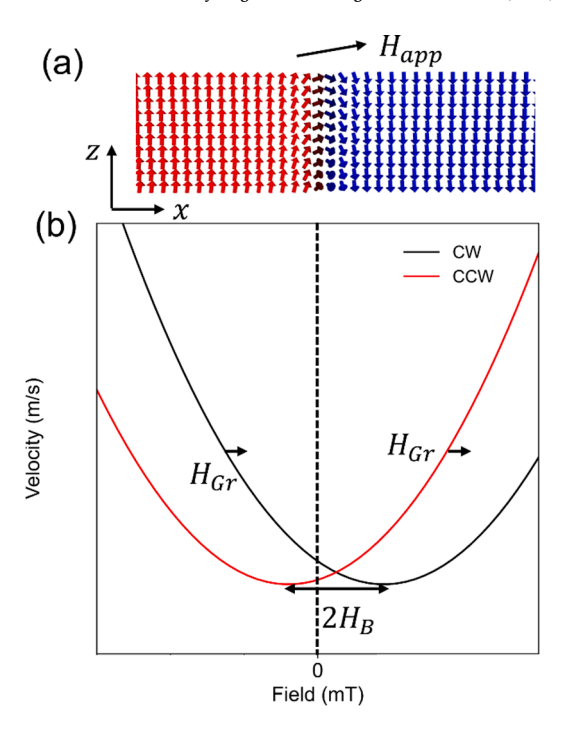


Fig. 1. (a) Schematic of simulation geometry showing applied field direction. The color represents the z-component of the magnetization. (b) Schematic of method used to determine effective fields following data fitting in the low field regime.

neighboring field values. Similar simulations were performed for no composition gradient but a non-zero DMI to compare the effects of M_s modulation with DMI. An effective field associated with the composition gradient or with DMI is measured by fitting the velocity-H $_{\! X}$ data at fields of H $_{\! X} \leq 100$ mT, wherein the in-plane field does not significantly tilt the magnetization in-plane, to

$$v = v_0 + A(H_x - (H_B + H_{Gr(DMI)}))^2$$
 (2)

where v is the domain wall velocity, v_0 describes the base velocity, A is a scaling constant associated with the total effective in-plane field, H_B is the effective field resulting from the Bloch chirality, and H_{Gr} is the effective field resulting from the gradient in M_s . For cases without a gradient but a non-zero DMI, the fitting is performed to extract H_{DMI} [40]. Determination of H_B and $H_{Gr(DMI)}$ from fitted data is then performed by noting that, for small values of H_x in which saturation of the domain wall magnetization along the field direction is minimal, $H_{Gr(DMI)}$ shifts velocity curves for both CW and CCW domains equally in the same direction, while H_B results in shifts of equal magnitude but opposite direction, as shown schematically in Fig. 1(b).

Simulations were also carried out up to $|H_x| \leq 500 \, \mathrm{mT}$ to estimate the effective field from high field velocity asymmetries following the method used for the determination of DMI from current induced domain wall motion [41-44], wherein the effective field is equal to the intersection of linear fits of the velocity at high fields. At these high fields the influence of the Bloch component of the magnetization is suppressed, and the wall can be described as predominantly Néel type.

The effect of a composition gradient on current driven domain wall motion via spin orbit torques (SOTs) was also explored. In simulations of SOT driven dynamics, only a damping-like torque was considered, and the spin injection was taken to be uniform throughout the film thickness, as would be approximately the case in systems with a bulk spin Hall effect. However, due to the non-uniform structure in the systems explored in this work, common injection schemes from interfaces with heavy metals or non-uniform current densities would significantly influence these results and the role of spatially varied current densities is

not explored. The current was modeled as a vertical spin current fully polarized along the y-axis with a current density $J=\pm 5\times 10^{10} A/m^2$.

2. Results and discussion

As indicated in the representative low field v-H_x curves, shown in Fig. 2(a) for a 40 nm thick film with saturation magnetization given by $M_s = 400 \pm 100 \, kA/m$, asymmetric domain wall velocities are observed in the presence of an in-plane magnetic field during the magnetization switching process. The data is well fit by Equation (1), with fitting allowing determination of H_B and H_{Gr}. Fig. 2(b) shows resulting effective fields at different film thicknesses with M_s = $400 \pm 100 \, kA/m.$ H_B shows no clear dependence with total film thickness at approximately 8 mT for all thicknesses. However, increasing the thickness leads to a large increase in H_{Gr} , from $2.1 \pm 1.5\,\text{mT}$ for the 10 nm thick film to $14.9 \pm 1.8\,\text{mT}$ for a 40 nm thick film. We then performed simulations with a fixed thickness of 40 nm and different variation in the saturation magnetization through the thickness to determine the role that the degree of variation in saturation magnetization played on the extracted effective fields, as shown in Fig. 2(c). Larger degrees of variation lead to larger H_{Gr} , reaching 25.2 \pm 1.4 mT in films with $M_s =$ $400 \pm 200 \, \text{kA/m}$. Reversing the sign of disorder leads to a sign change in H_{Gr}. This suggests that changing the direction of compositional nonuniformities in real systems will result in opposite signs of effective fields, identical to the expected behavior for gradient induced DMI,

further complicating the separation of these effects. Of further note, no significant change in H_{B} was observed, regardless of the degree of variation.

Additional simulations were performed to determine the effect of the average M_s . Here, the average M_s was varied with a fixed $\delta=100\,kA/m$. No notable effect on M_s was observed for H_{Gr} while H_B decreases significantly with decreasing M_s , as shown in Fig. 2(d). These results suggest that H_B predominantly depends on magnitude of M_s , and is independent of the uniformity of the film.

For $|H_x| > 100 \, \text{mT}$, asymmetric domain wall velocities are also observed for varying t, M_s , and δ as shown in Fig. 3(a-c). At these larger in-plane fields, only one Bloch chirality is stable, with a CCW or CW Bloch chirality for positive and negative H_x, respectively. H_{Gr} is identified to be equal to the field of intersection of the linear fittings of the high field $v - H_x$ curves for positive and negative H_x , respectively. As shown in Fig. 3(d), increasing the film thickness leads to a larger H_{Gr}, in line with the low field results. However, unlike the low field results, decreasing M_s while holding δ constant results in a notable increase in H_{Gr} (Fig. 3(e)). The mechanism for this qualitatively different behavior is unclear but may be due to changes in the internal domain wall structure during application of the in-plane field. Finally, the role of variation in saturation magnetization is found to follow similar trends to those found at low fields, with larger gradients resulting in larger H_{Gr}, shown in Fig. 3(f). In the high field and low Ms regime, for all simulations performed with a non-zero H_{Gr}, similar magnitude effective fields

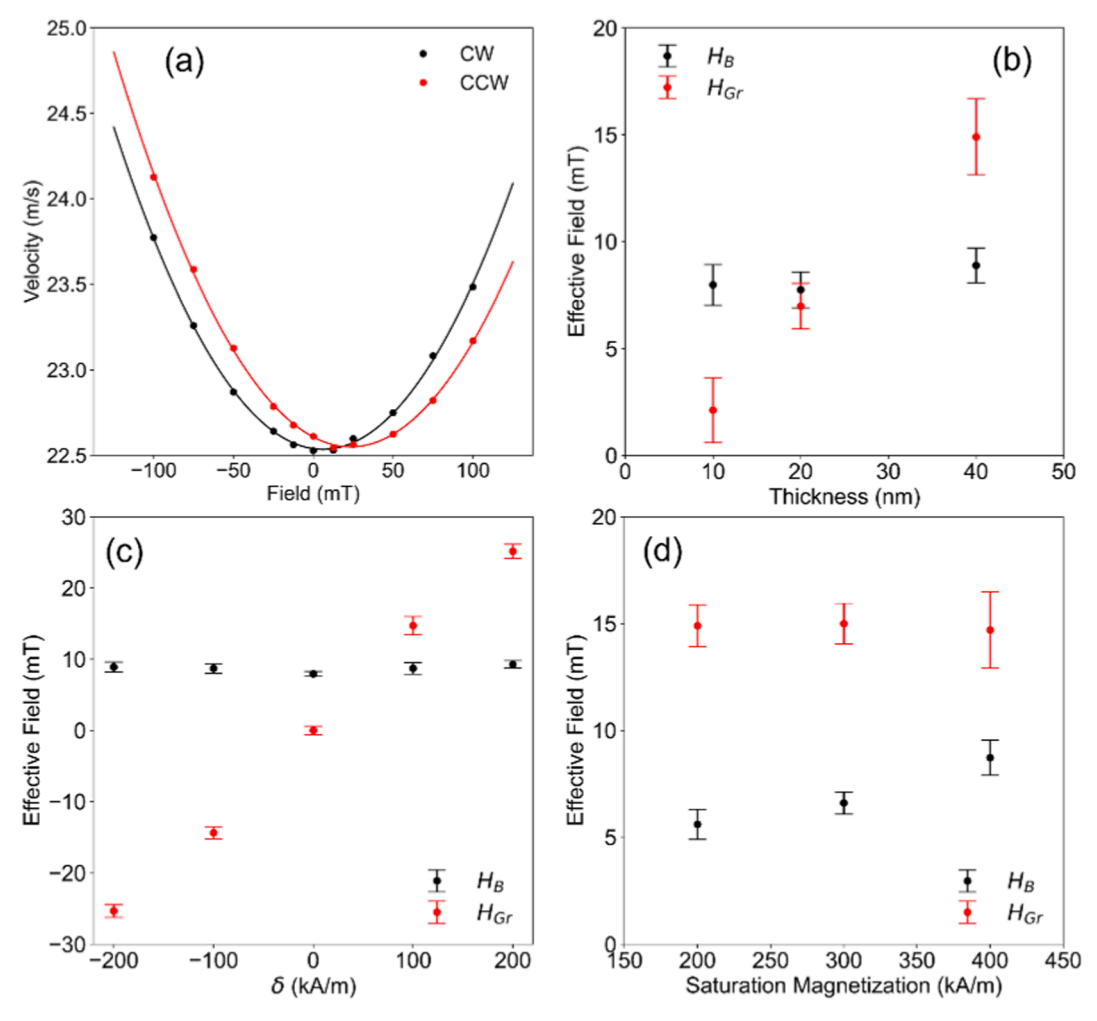


Fig. 2. (a) Representative $v-H_x$ curves for a 40 nm thick wire with $M_s=400\pm100\,k\text{A/m}$ and $H_z=2.5\,\text{mT}$. A clear offset is observed. Solid lines represent fits of the simulated data. (b) Effective fields vs. film thickness, with $M_s=400\pm100\,k\text{A/m}$. (c) Effective fields for varying δ with $t=40\,\text{nm}$ and $M_s=400\,k\text{A/m}$. (d) Role of average saturation magnetization vs. effective fields with $t=40\,\text{nm}$ and $\delta=100\,k\text{A/m}$. All effective fields are determined by fitting the low field region to Eq. (1).

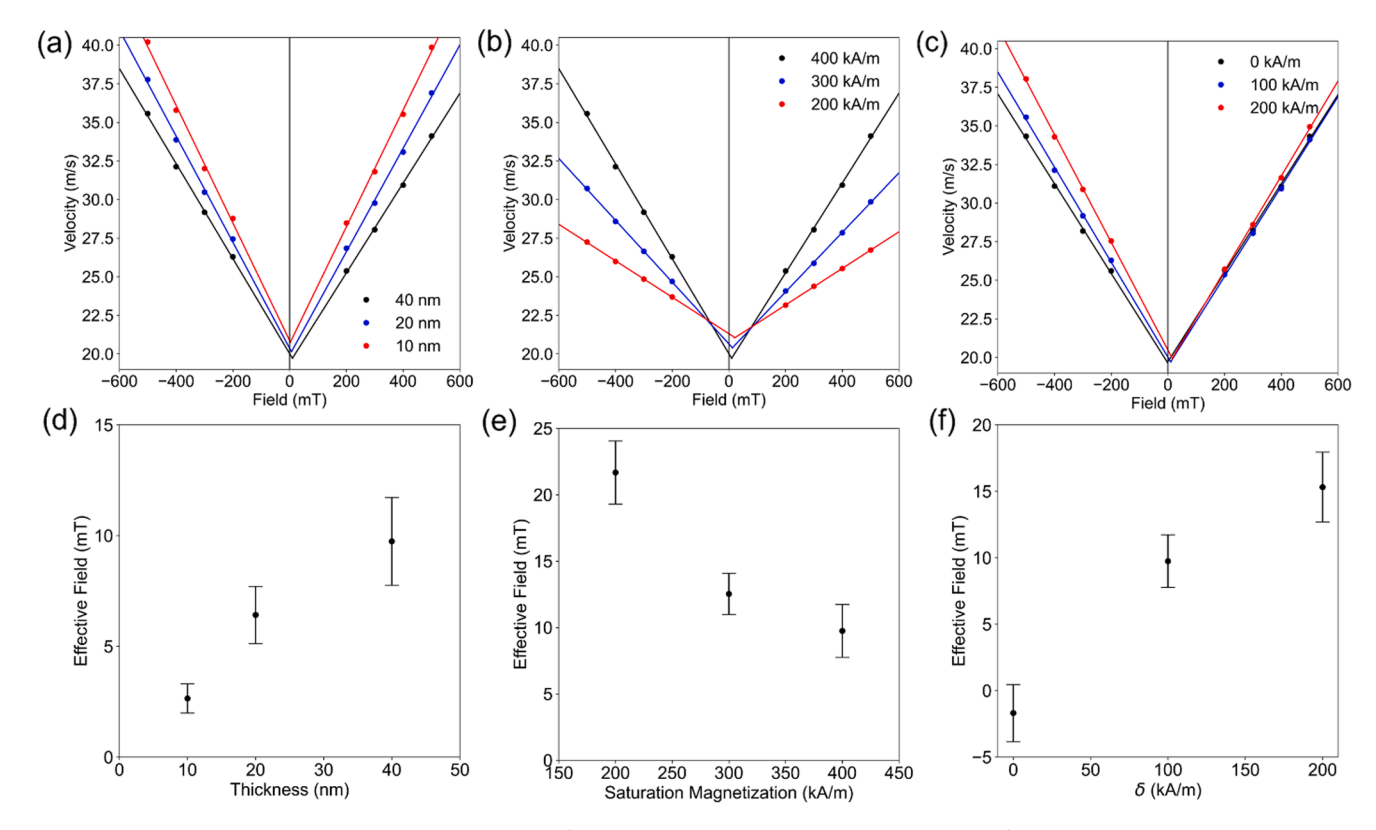


Fig. 3. High field $v-H_x$ curves for wires of (a) $M_s=400\pm100\,kA/m$ and varying t, (b) with $t=40\,nm$ and $\delta=100\,kA/m$ and varying average M_s , and (c) $t=40\,nm$ and $M_s=400+\delta$ with varying δ . Solid lines represent fits of the simulated data. (d-f) H_{Gr} extracted from (a-c), respectively.

were found as those in recent results for compositionally varied ferrimagnets and multilayers [31-33].

This asymmetry is a result of asymmetric Zeeman and demagnetization interactions, of which the demagnetization interaction preferentially selects a specific Néel chirality at top and bottom surfaces dependent on the relative orientation of neighboring domains. Due to the presence of the layer dependent saturation magnetization, energetic degeneracy of top and bottom surfaces is broken, as shown in Fig. 4(a) for a $t=40\,\mathrm{nm},\,M_s=400\pm200\,\mathrm{kA/m}$ wire. This asymmetry results in non-degenerate total domain wall energies, as shown in Fig. 4(b). The degree of the asymmetry scales with both magnitude of H_x and $\delta.$ As

domain wall velocities scale with domain wall energy density [43], this results in asymmetric velocities with respect to H_x .

To verify the similar behavior for H_{Gr} and H_{DMI} , we further carried out simulations of non-modulated wire structures with a DMI present and extracted the equivalent effective fields. At low H_x , while qualitatively similar results are obtained as those observed for compositionally non-uniform structures, a larger chirality dependent velocity offset is observed, as shown in Fig. 5(a). This is likely a result of dynamic effects which result in a preferred Bloch chirality[39]. Therefore, for comparison, we utilized high field velocities where the magnetization lies predominantly along the applied field direction, as shown in Fig. 5(b,c).

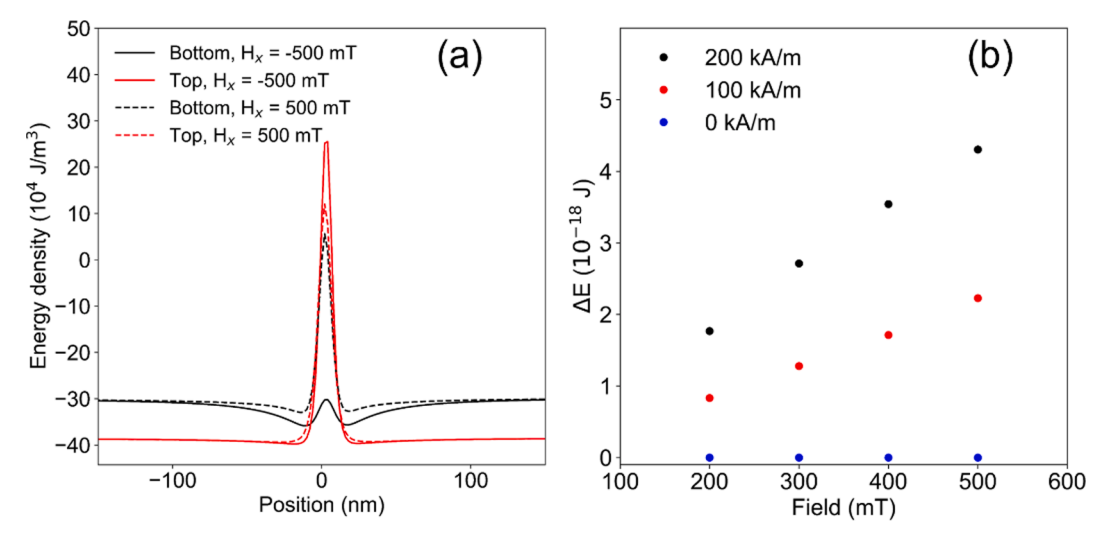


Fig. 4. (a) Energy density across a dynamic domain wall for $a=40\,\mathrm{nm},\,M_s=400\pm200\,\mathrm{kA/m}$ wire. Clear differences are observed with magnetic field direction, which result in asymmetric behavior with an in-plane magnetic field. (b) Asymmetry in total energy between positive and negative H_x , where $\Delta E=E(H_x)-E(-H_x)$ for the given δ . For larger δ , a larger asymmetry presents at a given field.

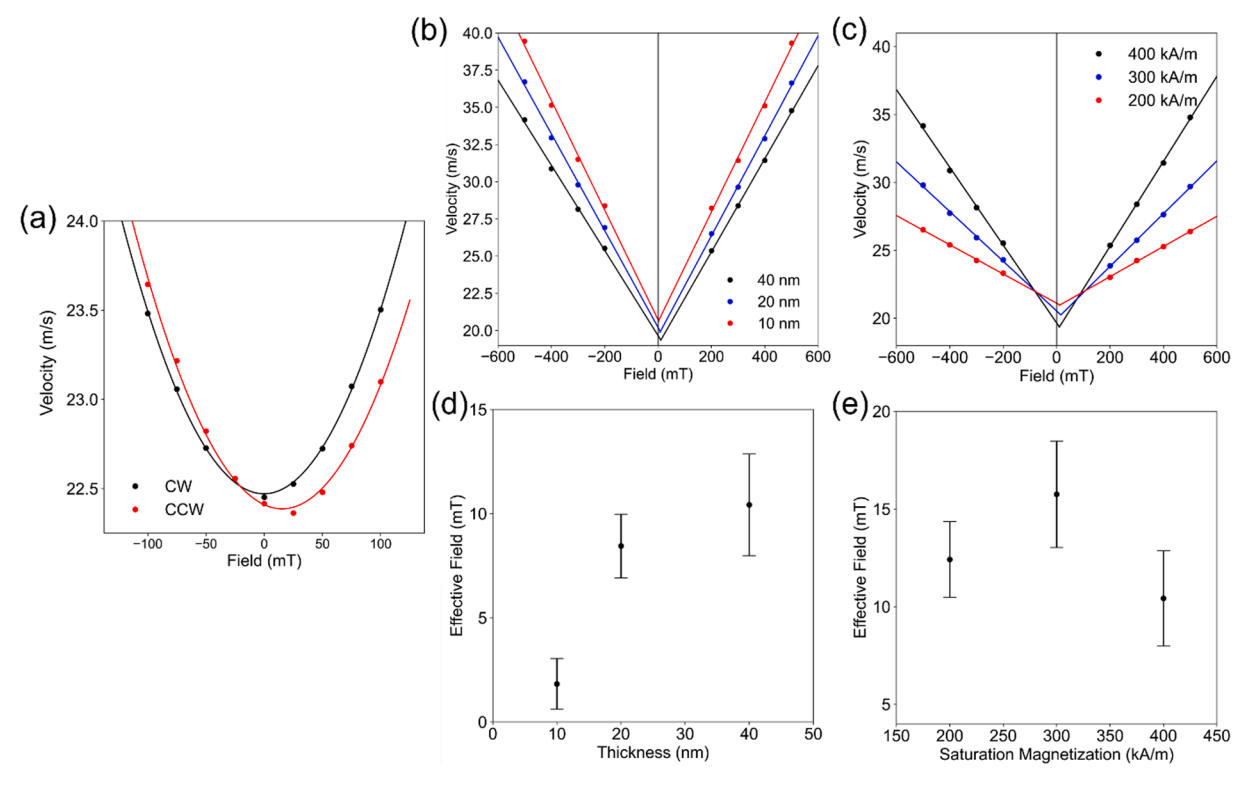


Fig. 5. (a) Low field $v-H_x$ curves for a 40 nm thick wire with $M_s=400\,kA/m$, $D=100\,\mu J/m^2$, and $H_z=2.5\,mT$ (b,c) High field $v-H_x$ curves for wires with (b) $M_s=400\,kA/m$, $D=100\,\mu J/m^2$, and varying t and (c) with $t=40\,nm$, $D=100\,\mu J/m^2$ and varying M_s . (d-e) DMI effective fields extracted from (b) and (c), respectively.

A DMI strength $D=100\,\mu J/m^2$ was used consistent with recent reports for compositional variation induced DMI. For both varying thickness and average saturation magnetization, $H_{DMI},$ shown in Fig. 5(d,e) is of similar magnitude as that of H_{Gr} determined solely due to a vertically inhomogeneous saturation magnetization.

The role of the composition gradient is also compared to DMI for SOT driven domain wall motion by determining the domain wall velocities as a function of H_x for opposite current densities. For SOT driven domain walls in ultrathin films with DMI, $H_{\rm DMI}$ is defined as the x-intercept of the $v-H_x$ curve and is identical for J>0 and J<0 [41,44,45]. Like the field driven case, $H_{\rm Gr(DMI)}$ shifts the $v-H_x$ curves for both CW and CCW domains equally in the same direction, while H_B results in shifts of equal magnitude but opposite direction. By noting the x-intercept for both chiralities, $H_{\rm Gr(DMI)}$ and H_B may be extracted. As SOT scales inversely proportional to M_x [38,46], current driven motion more strongly reflects

the influence of Néel chirality at the surface with lower M_s in the compositionally varied system. However, this scaling is complicated by the fact that the extent of the Néel chirality for the low M_s surface is smaller than that of the high M_s surface, as demonstrated in Fig. 6(a), which may lead to a reduced magnitude of $H_{\rm Gr}$. Additional complications arise when extracting DMI from asymmetric SOT driven domain wall motion due to the influence of SOT on the structure of the domain wall itself [47], further impacting the current driven dynamics, including potential variations that vary with the magnitude of the current density and were not explored in this work. For the current densities studied in this work, $H_{\rm Gr}$ and $H_{\rm DMI}$ result in drastically different asymmetries, as shown in Fig. 6(b,c), with the magnitude of asymmetry resulting from δ drastically reduced while the influence of the Bloch chirality is readily apparent.

The effects of varying film thickness and average saturation

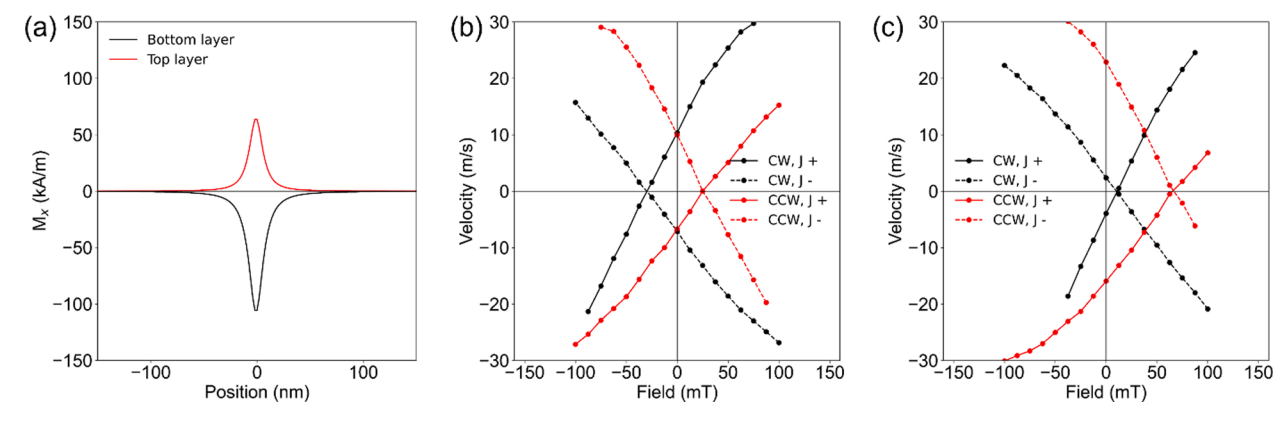


Fig. 6. (a) Net x-component of the magnetization along the top and bottom layers of a film with $t=20\,\mathrm{nm}$ and $M_s=400\pm100\,\mathrm{kA/m}$ showing the asymmetry between top and bottom layers. No external field or current is applied. (b) $v-H_x$ curves for wires with $t=20\,\mathrm{nm}$ and $M_s=400\pm100\,\mathrm{kA/m}$ for both positive (J+) and negative (J-) current densities. (c) Same as (b), but with $D=100\,\mu\mathrm{J/m^2}$ and no magnetization gradient.

magnetization for $\delta = 100 \,\mathrm{kA/m}$ are shown in Fig. 7a,b. Increasing M_s results in a larger asymmetry. This is due to the increase in demagnetization energies leading to an enhancement of Néel chirality at top and bottom surfaces, and therefore increasing the influence of δ on SOT driven domain wall motion. Increasing t also results in a larger asymmetry due to the enhanced Néel caps in the domain boundary. Similar increases with thickness were observed in compositionally modulated ferrimagnets [31]. For films where $\delta = 0 \text{ kA/m}$ and $D = 100 \,\mu\text{J/m}^2$, the opposite scaling is observed, as the decrease in demagnetization fields result in a strong Néel chirality through the film thickness determined by the sign of D, and therefore a lower M_s or t results in a larger velocity asymmetry, as shown in Fig. 7(c,d). Of note, in thick films with a varying M_s , the scaling for SOT and field driven motion is different, and the estimated magnitude of effective fields varies significantly between the two estimations. The mechanism for this is possibly related to the complex, three-dimensional spin structure observed in this work [48]. Finally, it should be noted that the discrepancy between field and current driven results may also be a result of the complex velocity scaling that may occur with current induced domain wall motion. Particularly, it has been demonstrated that damping- and field-like torques may significantly modify domain wall structures, leading to a tilting of the magnetization aligned along the axis orthogonal to current flow, inducing tilts in the domain wall itself, and leading to scaling of asymmetries with current densities [49].

3. Conclusion

Our work suggests a potential means to explore whether recent results in ferrimagnets are due to a gradient induced DMI or simply variation in saturation magnetization resulting from structural inhomogeneity. Specifically, in rare earth/transition metal (RE/TM) ferrimagnets, the sign of DMI is expected to depend only on the direction of composition gradient, where the percent TM either increases or decreases through the film thickness [31]. However, if the asymmetries are the result of variation in magnetic properties other than DMI, by fixing the direction of composition gradient but varying either temperature or average composition through the magnetization compensation point, either top or bottom surface will coincide with low or high magnetization relative to the opposite surface. By changing temperature, the top or bottom surface may be selected to be low magnetization, while maintaining a constant composition profile. By measuring how the velocity asymmetry varies, as indicated in Fig. 2(c), it is possible to distinguish these effects and determine the origin of the asymmetry. Further, our results suggest that measurements of DMI using current driven velocity

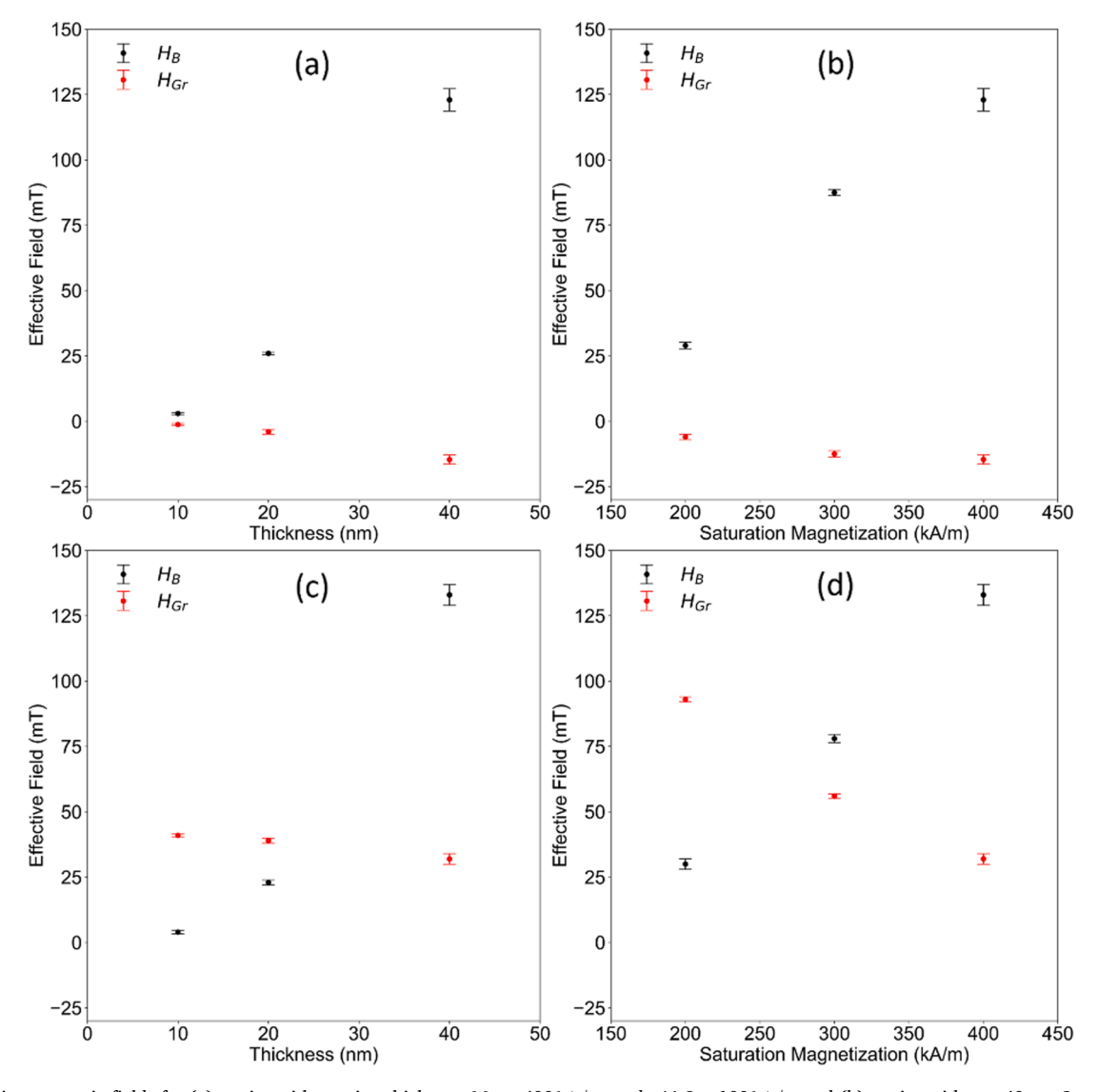


Fig. 7. Effective magnetic fields for (a) a wire with varying thickness, $M_s = 400\,k\text{A/m}$, and with $\delta = 100\,k\text{A/m}$ and (b) a wire with $t = 40\,n\text{m}$, $\delta = 100\,k\text{A/m}$ and varying M_s . (c,d) show the same as (a,b) but with $\delta = 0\,k\text{A/m}$ and $D = 100\,\mu\text{J/m}^2$.

asymmetries may be more robust to compositional variation due to the lower effective fields introduced by variation in saturation magnetization, and therefore offer an alternative means to explore DMI in compositionally varied systems. However, due to variations in current injection schemes, non-uniform current densities in inhomogeneous materials, and complications arising from the interactions of spintorques with three-dimensional spin structures, this method introduces other complications not present for field driven measurements.

In summary, we have shown that a depth dependent saturation magnetization in thin films can result in significant asymmetries in domain wall velocities with respect to an in-plane applied field for both field and current driven domain wall motion. The depth dependence of magnetic properties was chosen to be on the same order as those which may be found in ferrimagnetic alloys, which have also been suggested to host a significant DMI due to depth dependent structural variation. However, as many measurements of DMI also often rely on measurements of asymmetric domain wall velocities, our work suggests an alternative explanation that must be accounted for. We have further proposed possible methods in which to distinguish DMI from thickness dependent magnetic properties. Future experimental work considering both effects, as well as variation of other magnetic properties such as anisotropy and exchange stiffness, need to be carried out to determine the precise mechanism of the recently discovered asymmetric domain wall motion in ferrimagnets.

CRediT authorship contribution statement

Trae L. Staggers: Conceptualization, Investigation, Writing – review & editing. **Liyan Jacob:** Conceptualization, Writing – review & editing. **Shawn D. Pollard:** Conceptualization, Investigation, Visualization, Methodology, Writing – original draft, Supervision, Funding acquisition.

Declaration of Competing Interest

The authors declare that they have no known competing financial interests or personal relationships that could have appeared to influence the work reported in this paper.

Acknowledgements

Funding from the NSF under grant ECCS-2138271 is gratefully acknowledged.

References

- [1] M.J. Benitez, A. Hrabec, A.P. Mihai, T.A. Moore, G. Burnell, D. McGrouther, C. H. Marrows, S. McVitie, Magnetic microscopy and topological stability of homochiral Néel domain walls in a Pt/Co/AlOx trilayer, Nat Commun. 6 (1) (2015), https://doi.org/10.1038/ncomms9957.
- [2] A. Fert, N. Reyren, V. Cros, Magnetic skyrmions: advances in physics and potential applications, Nature Reviews Materials. 2 (2017) 17031, https://doi.org/10.1038/ natrevmats.2017.31.
- [3] W. Legrand, J.-Y. Chauleau, D. Maccariello, N. Reyren, S. Collin, K. Bouzehouane, N. Jaouen, V. Cros, A. Fert, Hybrid chiral domain walls and skyrmions in magnetic multilayers. Science. Advances. 4 (2018) eaat0415.
- [4] X. Zhang, Y. Zhou, M. Ezawa, Magnetic bilayer-skyrmions without skyrmion Hall effect, Nature Communications. 7 (2016) 10293, https://doi.org/10.1038/ ncomms10293.
- [5] S. Woo, K.M. Song, X. Zhang, Y. Zhou, M. Ezawa, S. Finizio, J. Raabe, J.W. Choi, B.-C. Min, H.C. Koo, J. Chang, Current-driven dynamics and inhibition of the skyrmion Hall effect of ferrimagnetic skyrmions in GdFeCo films, Nat Commun. 9 (2018) 959.
- [6] W. Jiang, X. Zhang, G. Yu, W. Zhang, X. Wang, M. Benjamin, Jungfleisch, J. Pearson, X. Cheng, O. Heinonen, K.L. Wang, Y. Zhou, A. Hoffmann, S.E. te, Velthuis, Direct Observation of the Skyrmion Hall Effect, Nature Physics. 13 (2) (2017) 162–169.
- [7] K. Zeissler, S. Finizio, C. Barton, A.J. Huxtable, J. Massey, J. Raabe, A. V. Sadovnikov, S.A. Nikitov, R. Brearton, T. Hesjedal, G. van der Laan, M. C. Rosamond, E.H. Linfield, G. Burnell, C.H. Marrows, Diameter-independent skyrmion Hall angle observed in chiral magnetic multilayers, Nature, Communications. 11 (1) (2020), https://doi.org/10.1038/s41467-019-14232-9.

- [8] K.-W. Kim, K.-W. Moon, N. Kerber, J. Nothhelfer, K. Everschor-Sitte, Asymmetric skyrmion Hall effect in systems with a hybrid Dzyaloshinskii-Moriya interaction, Physical Review B. 97 (2018), 224427, https://doi.org/10.1103/ PhysRevB 97 224427
- [9] M. Heigl, S. Koraltan, M. Vaňatka, R. Kraft, C. Abert, C. Vogler, A. Semisalova, P. Che, A. Ullrich, T. Schmidt, J. Hintermayr, D. Grundler, M. Farle, M. Urbánek, D. Suess, M. Albrecht, Dipolar-stabilized first and second-order antiskyrmions in ferrimagnetic multilayers, Nat Commun 12 (1) (2021).
- [10] F. Zheng, H. Li, S. Wang, D. Song, C. Jin, W. Wei, A. Kovács, J. Zang, M. Tian, Y. Zhang, H. Du, R.E. Dunin-Borkowski, Direct Imaging of a Zero-Field Target Skyrmion and Its Polarity Switch in a Chiral Magnetic Nanodisk, Physical Review Letters. 119 (2017), 197205, https://doi.org/10.1103/PhysRevLett.119.197205.
- [11] D. Capic, D.A. Garanin, E.M. Chudnovsky, Stability of biskyrmions in centrosymmetric magnetic films, Physical Review B. 100 (2019), 014432, https://doi.org/10.1103/PhysRevB.100.014432.
- [12] B. Göbel, J. Henk, I. Mertig, Forming individual magnetic biskyrmions by merging two skyrmions in a centrosymmetric nanodisk, Sci Rep 9 (1) (2019).
- [13] R. Tomasello, E. Martinez, R. Zivieri, L. Torres, M. Carpentieri, G. Finocchio, A strategy for the design of skyrmion racetrack memories, Sci Rep. 4 (1) (2015), https://doi.org/10.1038/srep06784.
- [14] X. Zhang, G.P. Zhao, H. Fangohr, J.P. Liu, W.X. Xia, J. Xia, F.J. Morvan, Skyrmionskyrmion and skyrmion-edge repulsions in skyrmion-based racetrack memory, Sci Rep. 5 (2015) 7643, https://doi.org/10.1038/srep07643.
- [15] V.L. Zhang, C.G. Hou, K. Di, H.S. Lim, S.C. Ng, S.D. Pollard, H. Yang, M.H. Kuok, Eigenmodes of Néel skyrmions in ultrathin magnetic films, AIP Advances. 7 (2017) 055212. https://doi.org/10.1063/1.4983806.
- [16] T. Moriya, Anisotropic Superexchange Interaction and Weak Ferromagnetism, Physical, Review. 120 (1960) 91–98, https://doi.org/10.1103/PhysRev.120.91.
- [17] T. Moriya, New Mechanism of Anisotropic Superexchange Interaction, Physical Review Letters. 4 (1960) 228–230, https://doi.org/10.1103/PhysRevLett.4.228.
- [18] I. Dzyaloshinsky, A thermodynamic theory of "weak" ferromagnetism of antiferromagnetics, Journal of Physics and Chemistry of Solids. 4 (1958) 241–255, https://doi.org/10.1016/0022-3697(58)90076-3.
- [19] K. Di, V.L. Zhang, H.S. Lim, S.C. Ng, M.H. Kuok, J. Yu, J. Yoon, X. Qiu, H. Yang, Direct Observation of the Dzyaloshinskii-Moriya Interaction in a Pt/Co/Ni Film, Physical Review Letters. 114 (2015), 047201, https://doi.org/10.1103/ PhysRevLett.114.047201.
- [20] S.-G. Je, D.-H. Kim, S.-C. Yoo, B.-C. Min, K.-J. Lee, S.-B. Choe, Asymmetric magnetic domain-wall motion by the Dzyaloshinskii-Moriya interaction, Physical Review B. 88 (2013), 214401, https://doi.org/10.1103/PhysRevB.88.214401.
- [21] H. Yang, A. Thiaville, S. Rohart, A. Fert, M. Chshiev, Anatomy of Dzyaloshinskii-Moriya Interaction at Co / Pt Interfaces, Physical Review Letters. 115 (2015), 267210, https://doi.org/10.1103/PhysRevLett.115.267210.
- [22] K. Di, V.L. Zhang, H.S. Lim, S.C. Ng, M.H. Kuok, X. Qiu, H. Yang, Asymmetric spin-wave dispersion due to Dzyaloshinskii-Moriya interaction in an ultrathin Pt/CoFeB film, Applied Physics Letters. 106 (2015) 052403. https://doi.org/10.1063/1.4907173.
- [23] J. Yu, X. Qiu, Y. Wu, J. Yoon, P. Deorani, J.M. Besbas, A. Manchon, H. Yang, Spin orbit torques and Dzyaloshinskii-Moriya interaction in dual-interfaced Co-Ni multilayers, Scientific Reports. 6 (1) (2016), https://doi.org/10.1038/srep32629.
- [24] M. Belmeguenai, J.-P. Adam, Y. Roussigné, S. Eimer, T. Devolder, J.-V. Kim, S. M. Cherif, A. Stashkevich, A. Thiaville, Interfacial Dzyaloshinskii-Moriya interaction in perpendicularly magnetized Pt/Co/AlO x ultrathin films measured by Brillouin light spectroscopy, Physical Review B. 91 (2015), 180405, https://doi.org/10.1103/PhysRevB.91.180405.
- [25] S.D. Pollard, J.A. Garlow, J. Yu, Z. Wang, Y. Zhu, H. Yang, Observation of stable Néel skyrmions in cobalt/palladium multilayers with Lorentz transmission electron microscopy, Nature Communications. 8 (1) (2017), https://doi.org/10.1038/ ncomms14761.
- [26] S. Kim, P.H. Jang, D.H. Kim, M. Ishibashi, T. Taniguchi, T. Moriyama, K.J. Kim, K. J. Lee, T. Ono, Magnetic droplet nucleation with a homochiral Néel domain wall, Physical Review B. 95 (2017), 220402, https://doi.org/10.1103/PhysRevB.95.220402.
- [27] S. Zhang, J. Zhang, Y. Wen, E.M. Chudnovsky, X. Zhang, Determination of chirality and density control of Néel-type skyrmions with in-plane magnetic field, Communications Physics. 1 (2018) 36, https://doi.org/10.1038/s42005-018-0040.5
- [28] J.-Y. Chauleau, W. Legrand, N. Reyren, D. Maccariello, S. Collin, H. Popescu, K. Bouzehouane, V. Cros, N. Jaouen, A. Fert, Chirality in Magnetic Multilayers Probed by the Symmetry and the Amplitude of Dichroism in X-Ray Resonant Magnetic Scattering, Physical Review Letters. 120 (2018), 037202, https://doi. org/10.1103/PhysRevLett.120.037202.
- [29] J.A. Garlow, S.D. Pollard, M. Beleggia, T. Dutta, H. Yang, Y. Zhu, Quantification of Mixed Bloch-Néel Topological Spin Textures Stabilized by the Dzyaloshinskii-Moriya Interaction in Co / Pd Multilayers, Physical Review Letters. 122 (2019), 237201, https://doi.org/10.1103/PhysRevLett.122.237201.
- [30] S.A. Montoya, S. Couture, J.J. Chess, J.C.T. Lee, N. Kent, D. Henze, S.K. Sinha, M.-Y. Im, S.D. Kevan, P. Fischer, B.J. McMorran, V. Lomakin, S. Roy, E.E. Fullerton, Tailoring magnetic energies to form dipole skyrmions and skyrmion lattices, Physical Review B. 95 (2017), 024415, https://doi.org/10.1103/PhysRevB 95 024415
- [31] D.H. Kim, M. Haruta, H.W. Ko, G. Go, H.J. Park, T. Nishimura, D.Y. Kim, T. Okuno, Y. Hirata, Y. Futakawa, H. Yoshikawa, W. Ham, S. Kim, H. Kurata, A. Tsukamoto, Y. Shiota, T. Moriyama, S.B. Choe, K.J. Lee, T. Ono, Bulk Dzyaloshinskii-Moriya interaction in amorphous ferrimagnetic alloys, Nature Materials. 18 (2019) 685–690, https://doi.org/10.1038/s41563-019-0380-x.

- [32] Z. Zheng, Y. Zhang, V. Lopez-Dominguez, L. Sánchez-Tejerina, J. Shi, X. Feng, L. Chen, Z. Wang, Z. Zhang, K. Zhang, B. Hong, Y. Xu, Y. Zhang, M. Carpentieri, A. Fert, G. Finocchio, W. Zhao, P. Khalili Amiri, Field-free spin-orbit torque-induced switching of perpendicular magnetization in a ferrimagnetic layer with a vertical composition gradient, Nat Commun 12 (1) (2021).
- [33] S. Krishnia, E. Haltz, L. Berges, L. Aballe, M. Foerster, L. Bocher, R. Weil, A. Thiaville, J. Sampaio, A. Mougin, Spin-Orbit Coupling in Single-Layer Ferrimagnets: Direct Observation of Spin-Orbit Torques and Chiral Spin Textures, Phys. Rev. Applied. 16 (2021) 24040, https://doi.org/10.1103/ PhysRevApplied.16.024040.
- [34] X. Xie, X. Zhao, Y. Dong, X. Qu, K. Zheng, X. Han, X. Han, Y. Fan, L. Bai, Y. Chen, Y. Dai, Y. Tian, S. Yan, Controllable field-free switching of perpendicular magnetization through bulk spin-orbit torque in symmetry-broken ferromagnetic films, Nature Communications. 12 (2021) 2473, https://doi.org/10.1038/s41467-021-22819-4.
- [35] A. Vansteenkiste, J. Leliaert, M. Dvornik, M. Helsen, F. Garcia-Sanchez, B. van Waeyenberge, The design and verification of MuMax3, AIP Advances. 4 (2014) 107133. https://doi.org/10.1063/1.4899186.
- [36] A. Vansteenkiste, B. van de Wiele, MUMAX: A new high-performance micromagnetic simulation tool, Journal of Magnetism and Magnetic Materials. 323 (2011) 2585–2591, https://doi.org/10.1016/j.jmmm.2011.05.037.
- [37] L. You, R.C. Sousa, S. Bandiera, B. Rodmacq, B. Dieny, Co/Ni multilayers with perpendicular anisotropy for spintronic device applications, Applied Physics Letters. 100 (2012) 172411. https://doi.org/10.1063/1.4704184.
- [38] R. Mishra, J. Yu, X. Qiu, M. Motapothula, T. Venkatesan, H. Yang, Anomalous Current-Induced Spin Torques in Ferrimagnets near Compensation, Physical Review Letters. 118 (2017), 167201, https://doi.org/10.1103/ PhysRevLett.118.167201.
- [39] M. Kitcher, M. de Graef, V. Sokalski, Deterministic switching of Bloch chirality in magnetic skyrmions: the Dzyaloshinskii astroid, (2021). https://arxiv.org/abs/ 2109.04499v1.
- [40] K.-J. Kim, Y. Yoshimura, T. Okuno, T. Moriyama, S.-W. Lee, K.-J. Lee, Y. Nakatani, T. Ono, Observation of asymmetry in domain wall velocity under transverse

- magnetic field, APL Materials. 4 (2016) 032504. https://doi.org/10.1063/
- [41] K.-S. Ryu, L. Thomas, S.-H. Yang, S. Parkin, Chiral spin torque at magnetic domain walls, Nat Nanotechnol. 8 (2013) 527–533, https://doi.org/10.1038/ pages 2013 105
- [42] S.A. Siddiqui, J. Han, J.T. Finley, C.A. Ross, L. Liu, Current-Induced Domain Wall Motion in a Compensated Ferrimagnet, Physical Review Letters. 121 (2018), 057701, https://doi.org/10.1103/PhysRevLett.121.057701.
- [43] A. Hrabec, N.A. Porter, A. Wells, M.J. Benitez, G. Burnell, S. McVitie, D. McGrouther, T.A. Moore, C.H. Marrows, Measuring and tailoring the Dzyaloshinskii-Moriya interaction in perpendicularly magnetized thin films, Physical Review B. 90 (2014), 020402, https://doi.org/10.1103/ PhysRevB.90.020402.
- [44] G.V. Karnad, F. Freimuth, E. Martinez, R. Lo Conte, G. Gubbiotti, T. Schulz, S. Senz, B. Ocker, Y. Mokrousov, M. Kläui, Modification of Dzyaloshinskii-Moriya-Interaction-Stabilized Domain Wall Chirality by Driving Currents, Physical Review Letters. 121 (14) (2018), 147203, https://doi.org/10.1103/PHYSREVLETT.121.147203.
- [45] D. Bang, H. Awano, High efficiency of the spin-orbit torques induced domain wall motion in asymmetric interfacial multilayered Tb/Co wires, Journal of Applied Physics. 117 (2015) 17D916, https://doi.org/10.1063/1.4916819.
- [46] K. Ueda, M. Mann, P.W.P. de Brouwer, D. Bono, G.S.D. Beach, Temperature dependence of spin-orbit torques across the magnetic compensation point in a ferrimagnetic TbCo alloy film, Physical Review B. 96 (2017) 064410. https://doi. org/10.1103/PHYSREVB.96.064410.
- [47] Y. Zhang, S. Luo, X. Yang, C. Yang, Spin-orbit-torque-induced magnetic domain wall motion in Ta/CoFe nanowires with sloped perpendicular magnetic anisotropy, Sci Rep 7 (1) (2017).
- [48] D.Y. Kim, D.H. Kim, S.B. Choe, Intrinsic asymmetry in chiral domain walls due to the Dzyaloshinskii-Moriya interaction, Applied Physics Express. 9 (2016) 053001. https://doi.org/10.7567/APEX.9.053001.
- [49] M. Baumgartner, P. Gambardella, Asymmetric velocity and tilt angle of domain walls induced by spin-orbit torques, Applied Physics Letters. 113 (2018) 242402. https://doi.org/10.1063/1.5063456.